Korean J. Chem. Eng., 36(4), 529-539 (2019)
DOI: 10.1007/s11814-018-0217-3

pISSN: 0256-1115
eISSN: 1975-7220

Phenol removal from aqueous solution using amino modified silica nanoparticles

Sayed Saleh*,,†, Alaa Younis***, Reham Ali**,****, and Eman Elkady*****

*Chemistry Branch, Department of Science and Mathematics, Faculty of Petroleum and Mining Engineering, Suez University, 43721 Suez, Egypt
**Chemistry Department, Faculty of Science, Qassim University, Buraidah, KSA
***Aquatic Environment Department, Faculty of Fish Resources, Suez University, 43518 Suez, Egypt
****Chemistry Department, Faculty of Science, Suez University, 43518 Suez, Egypt
*****Marine Chemistry lab, National Institute of Oceanography & Fisheries, Suez, Egypt
(*Received 18 September 2018 • accepted 20 December 2018*)

Abstract−Phenols constitute a widespread class of water pollutants that are generated from many industries and are known to cause a significant threat to the aquatic environment. Phenols are, therefore, considered as dangerous pollutants by global international quality organizations. This has led to a growing demand for an efficient technology for phenol removal from wastewater. Different sizes of amino-modified silica nanoparticles (SiNPs) were synthesized with 10-40 nm in diameter (AMS-10 to 40), and their properties were characterized in terms of size and surface modification using transmission electron microscope (TEM), dynamic light scattering (DLS), zeta potential, elemental analyses (C, H, N), thermal gravimetric analysis (TGA) and Fourier transform infra-red (FTIR). The adsorption process was carried out utilizing batch mode experiment; the influence of various factors including pH of the medium, the contact time, the initial concentration of the adsorbate and the dose of the adsorbent on the phenol adsorption efficiency of SiNPs of various sizes were investigated. Phenol removal efficiency was found to be size-dependent, such that the phenol adsorption capacity of the SiNPs was in the following order: AMS-10>AMS-20>AMS-30>AMS-40 nm. The adsorption capacity and binding coefficient were calculated to be 35.2 mg/g and 0.192 mg/L, respectively, for AMS-10. The amino-modified SiNPs were found to be promising adsorbents for the phenol ions removal from the aqueous medium.

Keywords: Silica Nanoparticles, Surface Modification, Phenol Removal, Water Treatment

INTRODUCTION

Phenols are one of the major constituents of industrial wastewater that are related to coal gasification, pharmaceuticals, gasoline, plastic, disinfectant, rubber proofing, and steel industries as well as agricultural run-off and domestic wastewaters [1]. There has been increasing interest in the toxicological and environmental effects of organic compounds, especially phenolic pollutants due to their widespread occurrence and relative frequency in the aquatic environment [2,3]. Due to the stability and high solubility of phenolic compounds in water, these compounds pose a potential toxicity threat to aquatic organisms through accumulation in their food chains. Typically, contaminated waters from industrial discharge usually contain phenol in concentrations ranging from 0.1-6, 800 mg/L [4]. The acceptable level of phenol in surface water should limited to 3.5 mg/L to protect people from drinking contaminated water [5]. Because of their toxic characteristics as well as their possible biodegradation, phenolic compound removal from contaminated water is vital [6]. Attention has been paid to the development and implementation of environmentally and economically efficient techniques of phenolic compounds removal from wastewater.

Several adsorption techniques have been utilized for water purification based large-scale adsorption approaches. These technologies have a great impact in wastewater treatment such as reverse osmosis [7,8], membrane separation [9,10], electrochemical oxidation [11], solvent extraction [12], bioremediation [13,14], wet air oxidation [15,16], photo catalytic degradation [17,18] and chemical coagulation [19]. Furthermore, the production of an economic, efficient and instant water treatment at a large scale has attracted more attention. Among these techniques, solid phase extraction (SPE) has been increasingly utilized as a simple route for removal of pollutants. The massive development of SPE has led to utilizing numerous types of materials or nanomaterials as solid phase extraction materials. SPE has been applied to numerous types of matrices such as serum, blood, urine and oil [20]. Also, the SPE technique proceeds based on several types of mechanisms such as electrostatic, cation-anion interaction and hydrogen bonding. SPE is one of the best choices for wastewater treatment. It involves the ability of certain nano, micro or coarse sized solid materials to accumulate specific molecules onto their surfaces from solution perfectly. Several parameters have been investigated for optimizing the utility of nonconventional adsorbents in the treatment process of wastewater, including (a) adsorbate and adsorbent nature, (b) concentration of the adsorbate, (c) adsorbent dose, (d) contact time, (e) solution pH, and (f) particle size of adsorbent [21]. Thus, various non-conventional adsorbents like sawdust, rice husk ash, charcoal, fly ash and numerous types of fibers have been studied [22].

Different adsorbents such as biosorbents [23], zeolites [24], acti-

†To whom correspondence should be addressed.
E-mail: sayed.saleh@suezuniv.edu.eg

vated carbon [25], carbon nanotubes [26], clays [16], different polymers [27,28], ordered mesoporous carbon [29], synthetic resins [30,31], hollow mesoporous carbon spheres [31], and amine-modified mesoporous silica [32] have been recently studied. However, all of these have some disadvantages, such as the formation of toxic by-products in the aquatic environment. Despite the various adsorbent materials widely used for phenol removal, treatment using silicates or polymers offers an effective method for pollutant removal such as phenol from wastewater. Silicate particles show many advantages over other types of materials due to their high purity, enormous surface area, high adsorption capacity and ease of manufacturing [33]. Therefore, adsorption-based phenol removal remains one of the best treatment choices as it can commonly remove all phenol compounds in a very straightforward way.

Low cost and economic systems are needed for synthesis of silica nanoparticles (SiNPs) in addition to inert properties, safe use and resistant to bio-environment, making it a promising candidate and efficient adsorbent material to use in removal of toxic and waste compounds. These specified silica nanoparticles have not been used as adsorbent materials for phenol removal. Furthermore, (SiNPs) combine various beneficial properties such as excellent permeability [34], superior mechanical strength [35] and high chemical [36] and thermal stability [37]. Furthermore, their high surface area and surface activity increase their chance to efficiently remove toxic and harmful pollutants from the environment [38]. These biocompatible SiNPs are, therefore, used to remove chlorine, pesticides and heavy metals from water [39,40]. The diminutive size of the SiNPs, commonly up to 40 nm, results in a diverse surface area per unit volume, which renders them as spontaneous and highly reactive compounds compared to their micro or coarse sizes [41].

The present work's aim is to introduce and study amino functionalized SiNPs for phenol removal from aqueous solution. These particles were synthesized with different sizes (10-40 nm), and the resulting plain nanoparticles were modified to enhance the adsorption capability of the particles [42,43]. The influence of the particle size was investigated on phenol removal process. The removal efficiency of the different-sized SiNPs, 10-40 nm, showed significant variation towards phenol compounds due to alteration of surface area per unit volume. The amino modification of the SiNPs surface improves the surface characteristics, makes the particles more powerful, and raises the removal efficiency. Concerning other types of nanomaterials, SiNPs can be utilized to remove phenol from wastewater and reduce potential harm to the environment. The synthesized SiNPs showed very promising behavior in the phenol removal process from aqueous media using batch adsorption experiments. Therefore, they can be used with other pollutants to clean up other contaminants from water by SiNPs.

MATERIALS AND METHODS

1. Chemicals

All reagents were purchased from Sigma-Aldrich, and used without any purification. All solutions were prepared using bi-distilled water. Tetraethyl orthosilicate (TEOS 98%), APTS (3-Aminopropyl) trimethoxysilane with purity 97%, ammonium hydroxide solution 33% (NH_3) were purchased and used as received from the Sigma Aldrich Company. Standard stock solutions of 1,000 mg L^{-1} of phenol were prepared in bi-distilled water and stored in brown glass bottles at −4 °C in the refrigerator. The working solutions were prepared from an aqueous phenol stock standard solution by diluting with bi-distilled water to the required concentrations.

2. Synthesis of Amino Functionalized Silica Nanoparticles

The amino modified SiNPs were synthesized by Stöber et al. [44], followed by seed growth technique. A solution mixture of 40 mL ethanol, 1 mL bi-distilled water and 1 mL of ammonia solution (25%) was prepared by stirring at 40 °C, for about 15 minutes, and after that 1.25 mL TEOS was added to the solution with slow stirring for 3 h at the same temperature. Then, 1 mL TEOS was added to the mixture and the stirring was continued for further 30 minutes. For introducing the amino groups to the nanoparticles surface, 100 μL of APTS was combined with the reaction mixture and stirred for another 3 h under the same stirring rate, 150 rpm, at 40 °C. The resulting colloidal solution was cooled to room temperature and matured for at least eight days to allow the particles to grow symmetrically [45].

To get efficient reproducibility of SiNPs batches, the reaction temperature and the stirring rate should be kept constant. Additional times of the precursor to the resulting solution are essential and critical. Moreover, the time intervals between TEOS portions should be kept to an accurate time schedule as illustrated. The nanoparticle growth period should be constant for all batches within the range of 8-9 days.

3. Growth Control of Silica Nanoparticles

Different size amino-SiNPs were synthesized utilizing different portions of TEOS and bi-distilled water. The size and reactant concentrations are summarized Table 1.

4. Materials Characterization

Different techniques were used to characterize the modified SiNPs based on their size and surface modification. Transmission electron microscopy (TEM) was performed on TEM; in order to prepare SiNPs samples for TEM analysis, centrifugation and washing cycles is dispersed in absolute ethanol and a drop of silica suspension was transferred to the surface of a copper grid coated with carbon. The grid was left at room temperature for complete solvent evaporation, leaving only SiNPs on the grid surface. Operating at an acceleration voltage of 200 kV, the magnification used reached ×40,000 in order to view the small nanoparticles 40 nm in diameter and smaller. Images were taken for both a distant/perspective view and high magnification images of individual nanoparticles. Particle sizes and zeta potentials were characterized by dynamic light scattering (DLS) [46]. It can detect the particle sizes within range of from 0.6 nm to 6 μm; the studied nanoparticles were sus-

Table 1. The reactants concentrations of modified SiNPs

Sample	Size (nm)	Water (mL)	TEOS (mL) addition	
			1st Portion	2nd P.
AMS-10	10 nm	2	2.25	1.25
AMS-20	20 nm	1	1.25	1.0
AMS-30	30 nm	1	2.0	1.25
AMS-40	40 nm	1	3	1.25

pended in buffered aqueous medium at pH 6. Fourier transmission infra-red (FTIR) analysis was carried out on a Jasco FTIR-4100 Jasco-Japan instrument [47]. Elemental analysis was by using vario EL III Element Analyzer.

5. Batch Adsorption Experiments

To investigate the influence of different factors such as initial concentration, pH, contact time and adsorbent dose on the adsorption capacity of phenol onto SiNPs, all experiments based batch adsorption was performed in 40 mL stoppered conical flasks by wetting 25 mg of the SiNPs into 25 mL of aqueous solution, including phenol, then mechanically shaken in the dark at room temperature 25±2 °C. Batch experimental procedures were used to detect the influence of solution pH within range (3-10) on the phenol removal efficiency by SiNPs, and the pH values were appropriately controlled with 0.1 M HCl or NaOH solution and measuring the pH with standardized pH meter. 25 mg of SiNPs was added to the aqueous solution containing 10, 20, 30 and 40 mg/L phenol in 100 mL Erlenmeyer flasks to investigate the influence of various phenol concentrations on the SiNPs adsorption efficiency (Scheme 1).

To investigate the influence of contact time, procedures of batch experiments were varied using the following shaking time intervals--1, 6, 12, 18 and 24 h--in the dark at neutral pH medium of 7.0, while the other factors including adsorbent dosage and initial concentration of phenol were maintained at constant values. The adsorption capacity of SiNPs to degrade phenol from aqueous solution was determined. The sorbent materials with the following concentrations (0.01, 0.02, 0.03, 0.04 and 0.05 g/25 mL) were used to investigate the sorbent dosage effect, and the other factors including pH, phenol concentration and contact time were kept constant. At the end of the adsorption process, measurements of the residual phenol concentrations in each solution were carried out with colorimetric methods using VIS/UV Spectrophotometer-19 (SCO-Tech, Germany) [48].

The adsorption of phenol from water into SiNPs was studied based on the difference in initial and final concentrations, respectively, when the equilibrium of adsorption process was established. To detect the efficiency of repeatability significantly, all the experiments were in triplicate and the obtained data were verified for reproducibility with error bars less than 5% in uptake. Negative controls (with no adsorbent) were concurrently achieved to investigate phenol ion deficiency through the adsorption. The removal efficiency percentage (E %) of phenol from aqueous solution based SiNPs was estimated utilizing the following equation:

$$E\,\% = \left[\frac{C_o - C_e}{C_o}\right] \times 100$$

where:

C_o: the initial concentrations, and C_e: the final concentrations of phenol in aqueous solution.

The adsorption capacity of phenol into SiNPs was estimated using the following equation:

$$q_t = \frac{(C_o - C_t)V}{m_s}$$

where q is the phenol quantity adsorbed in presence of the SiNPs expressed in mg/g. C_o and C_e are the initial and final equilibriums of phenol concentrations, respectively. m_s and V are weight of SiNPs and volume of solution, respectively.

6. Adsorption Isotherm Models

To determine the equilibrium relationship between the sorbate amount adsorbed on the surface of adsorbent and its equilibrium

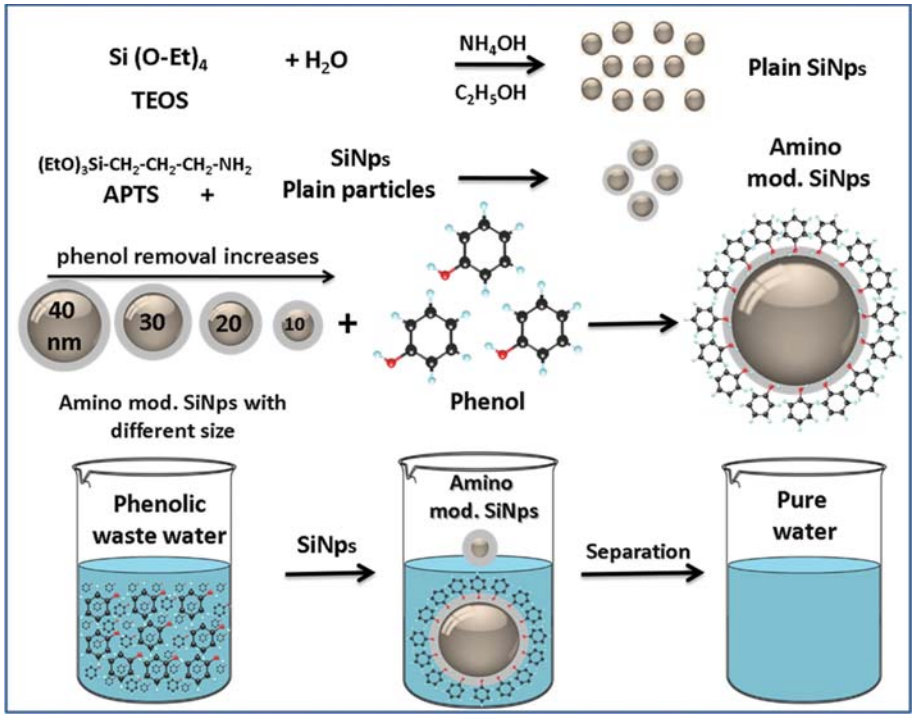

Scheme 1. Schematic of the phenol removal process using different size of amino modified SiNps.

concentrations in the aqueous medium under a constant temperature, adsorption isotherm studies were carried out at equilibrium conditions. The current adsorption data of phenol was studied by the Langmuir and Freundlich models according to the following equations:

$$\frac{C_e}{Q_e} = \frac{1}{Q_{max}K_L} + \frac{C_e}{Q_{max}}$$

$$\mathrm{Log}Q_e = \log K_f + \frac{1}{n}\mathrm{Log}C_e$$

where: Q_e (mg/g), amount adsorbed (mg/g). C_e (mg/L), equilibrium concentration of phenol in the liquid phase; Q_{max} (mg/g), maximum adsorption capacity. K_L, Langmuir constant. K_f and n are the Freundlich constants.

RESULTS AND DISCUSSION

1. Synthesis of the Different Size SiNPs

Recently, silane precursor (TEOS) was used to prepare SiNPs by either the Stöber method or microemulsion method (water in oil w/o) [44,49]. The silicate precursor in both methods undergoes hydrolysis, which results in the growth of the nanoparticles. In case of the microemulsion method, a surfactant and oil are used to form the micelles. To obtain the nanoparticles, several cycles of washing-centrifugation are necessary. These washing cycles can lead to an aggressive aggregation. However, the Stöber method was chosen, in this study, for the synthesis of SiNPs, as it does not need to use surfactant or oil.

The surface modification of SiNPs is normally accomplished by reacting the nanomaterials with the silane precursor in toluene solution under reflux [42]. However, this was found not to be suitable for the formation of mono-dispersed particles due to formation of particle aggregates. Therefore, the one-pot method, which is based-on Stöber method, was used to synthesize the nanoparticles and to decrease the probability of particle aggregates. The methodology of the synthesis process was conducted on three stages: formation of nanoparticle seeds, addition of TEOS to the solution in order to form the shell surrounding the seeds, and finally introducing the silane active group.

According to the synthesis mechanism, base-catalyzed nucleation takes place via the condensation process of silicic acid into oligomeric chains. Moreover, these chains will combine, forming larger particles. Thus, the condensation process happens in a very short time with a high reaction rate in a single step. Also, the reaction goes from Si-OR without formation Si-OH in a separate step. Ammonia provides hydroxyl groups in an aqueous medium, which facilitates the condensation process through increasing the hydrogen bonds in the nucleation medium. With respect to ethanol and water and in presence of ammonia, water has the tendency to ionize faster than ethanol. Thus, nucleation will occur with bigger molecules in the presence of high water concentration but with less order of crosslinking. With increasing the ethanol concentration, this forms a smooth surface with more order of crosslinking. Finally, ammonia plays an important role as a source for hydroxyls, which considerably quenches the ionization energy, thus permitting for the production of more hydroxyls from ethanol and water ionization. Therefore, there is no other influence from the base and offers significant stability, as the number of hydroxyls on the surface of nanoparticles is dependable for particle stability not related to ammonia. Silica nanoparticles were synthesized based on other types of base [50].

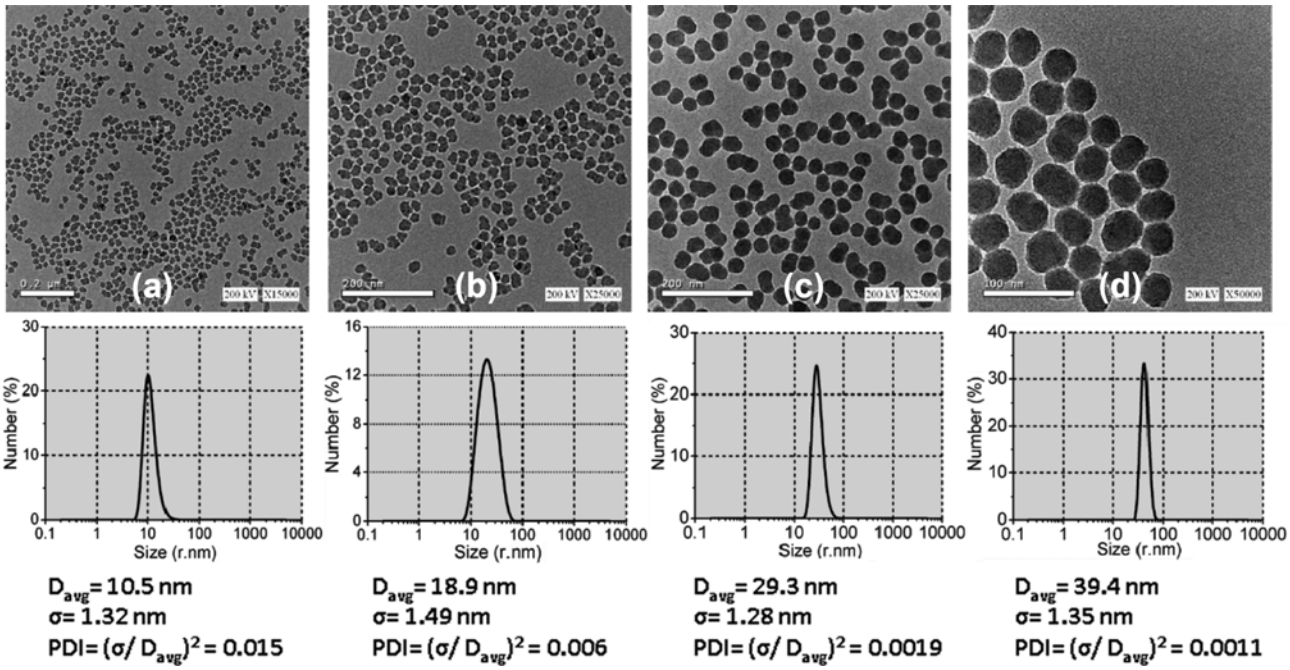

Fig. 1. Transmission electron microscopy images and differential light scattering DLS of amino modified SiNPs showing ((a), (b), (c) and (d)) images that represent AMS-10, AMS-20, AMS-30 and AMS-40, respectively.

Therefore, the concentrations of the ammonia and the ethanol (solvent) were kept constant, while the precursor/water ratio was varied during the synthesis of different types of SiNPs. Under such conditions, we managed to synthesize different sizes of SiNPs by varying the concentration of TEOS. Note that increasing the precursor concentration accelerated the nucleation process, yielding SiNPs with larger diameter: AMS-10, AMS-20 and AMS-30. However, upon increasing the molar concentration of water, the nucleation reactions (hydrolysis) were found to be preferred over the condensation reactions (growth). This, collectively, led to accelerating the growth rate of silica nano-seeds and led to a preferential synthesis of larger nanoparticles (AMS-40).

2. Characterization

The TEM images of SiNPs, shown in Fig. 1, indicate mono-dispersed amorphous nanoparticles with approximate size range of 10, 20, 30 and 40 nm. This is further supported by the differential light scattering (DLS) measurements, showing characteristic peaks within the same size range. Also, the small values of PDI (poly dispersion index) of all different modified silica nanoparticles indicate that all the samples are monodispersed (Fig. 1). Moreover, zeta potential measurements [42] showed that the surface charge of plain SiNPs was modified at pH 6 by introducing amino groups. Plain SiNPs are negatively charged at pH 6 due to the presence of dissociated silanol groups. The value of zeta potential of the plain particles was −28.7 mV. In contrast, the zeta potential value of amino modified SiNPs was found to be +28.9, +35.3, +39.3 and +46.1 mV for AMS-40, AMS-30, AMS-20 and AMS-10 respectively, due to the existence of positively charged amino groups at the particles' surface. This is evidence for the increasing of attached amino groups to surface of nanoparticles with decreasing particle size and consequently increasing surface area.

Conventional elemental analysis C, H, N was utilized to detect the chemical composition of SiNPs surfaces. The appearance of a definite amount of hydrogen in the plain sample, Table 2, is clearly related to adsorbed water molecules at the surface. In the modified sample, however, the presence of a definite amount of nitrogen provides evidence that the APTS have spontaneously reacted to the silanol surface group of the silica nanoparticles. Also, the existence of a significant percentage of carbon on the surface of amino modified silica nanoparticles is indicative of the presence of alkyl groups bound to the surface. Moreover, the nitrogen and carbon content on the surface of the silica nanoparticles decreased with increasing the size of the nanoparticles. This could be attributed to the increment of the surface area of the nanoparticles with decreasing the size, and this provided greater probability for attaching amino groups to the nanoparticle surface.

Table 2. Elemental characterization of silica nanoparticles

SiNPs type	% C	% H	% N	% S
Plain particles	0.28±0.010	0.19±0.030	Nil	0.00
AMS-10	5.04±0.010	0.90±0.043	1.04±0.035	0.00
AMS-20	4.32±0.010	0.78±0.035	0.89±0.030	0.00
AMS-30	3.91±0.010	0.70±0.030	0.81±0.032	0.00
AMS-40	3.72±0.010	0.66±0.038	0.74±0.034	0.00

The characteristics of the amino modified SiNPs were also proved utilizing FTIR analysis, Fig. 2(a). Comparing the FTIR of plain and modified SiNPs reveals a $\nu(NH_2)$ at 1,580 cm^{-1} with a ν(C-H) weak bands at 2,700 cm^{-1} in the modified particles. TGA analysis shows that the weight loss in case of modified nanoparticles is higher than that in case of plain particles. Besides, the weight loss of the modified particles decreased gradually with increasing the particle size, as shown in Fig. 2(b). Thus, the TGA and elemental analyses deliver insightful information about the surface modification of silica nanoparticles by amino groups and how this process depends on size and surface area of the synthesized nanoparticles. These behaviors indicate the presence of the carbon chain of the APTS group which is cross-linked to the inorganic silica matrix of the modified particles.

3. Adsorption Process

3-1. Contact Time Effect

The effective sorption time spent in adsorbate-adsorbent interaction is one of the critical parameters that define the efficiency of adsorption. To investigate the effect of contact time on the maximum uptake of phenol ions by SiNPs, the removal experiment was carried out as a function of contact time (1-24 h), while keeping pH, initial concentration and adsorbent dosage constant at 7, 10 mg/L and 1 mg/1 mL respectively. To ensure reproducibility, the experiment was carried out in triplicate. A gradual increase of the removal % of phenol was observed as the contact time increased from 1 h to 18 h, Fig. 3. Notably, no further increase was observed

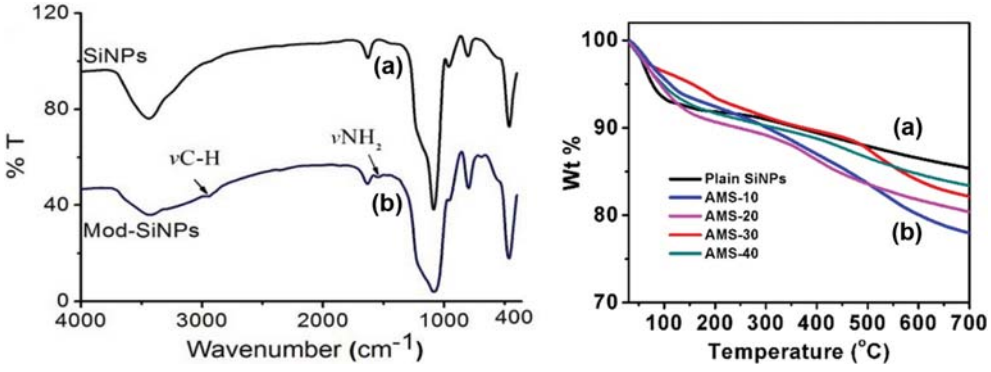

Fig. 2. FTIR and TGA analyses of SiNPs (a) plain NPs and (b) amino-modified NPs.

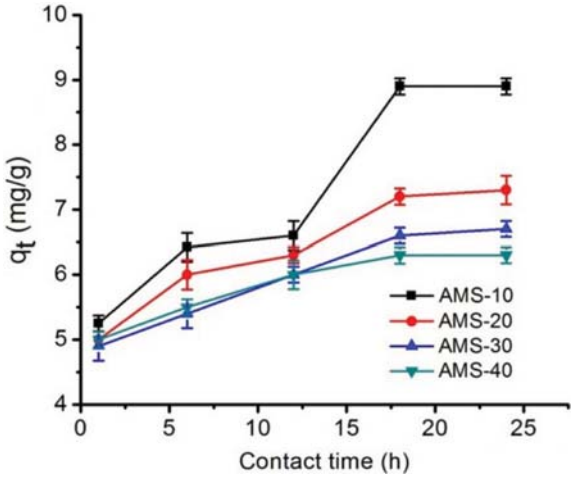

Fig. 3. The influence of contact time on the phenol adsorption capacity using SiNPs (Initial concentration=10 mg/L, dosage of adsorbent nanomaterials=1 mg/1 mL at pH=7).

at longer times. Adsorption rate of phenol ions on SiNPs was found to be in good agreement with previous studies for some adsorbents [23,51]. Bromophenol adsorption onto carbonaceous adsorbents resulting from solid fertilizers waste was conducted by Bhatnagar [52] and reached equilibrium after 8 h. This behavior can be attributed to the presence of enough vacant adsorption sites on the adsorbent during the first 18 h of adsorption, which is the time required to reach the adsorption equilibrium point. At this stage, the active sites on the adsorbents surfaces became saturated, and no more removal of the phenol ions from the aqueous media was carried out [53]. Furthermore, the adsorption efficiency of the AMS-10 sample was higher than other adsorbents at the same contact time. The increase in contact time, after approximately 12 h, led to a sharp increase in the removal efficiently of phenol ions on AMS-10. This behavior may also be due to the smaller average size of the AMS-10 sample with a higher surface area of adsorbent and

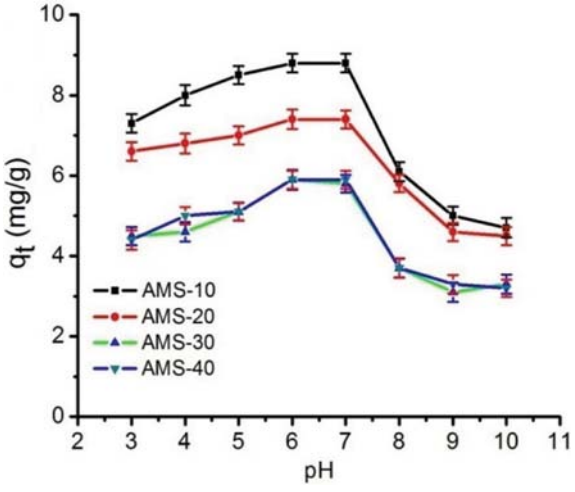

Fig. 4. Influence of pH on adsorption capacity of phenol using SiNPs (Initial concentration=10 mg/L, dosage of adsorbent=1 mg/1 mL and contact time=18 h).

total pore volume. This could be attributed to the phenol ions going deeper into the surface pores and consequently diminishing the boundary layer resistance of the silica layer [54].

3-2. Study of the Effect of Solution pH

The pH value of solution is an essential variable in the adsorption capacity of phenol from wastewater. Fig. 4 shows the effect of pH of solution on the adsorption efficiency of phenol by SiNPs at pH values ranging between 3 and 10, while keeping other factors such as adsorbent dosage, contact time and initial concentration constant at 1 mg/1 mL, 18 h and 10 mg/L, respectively. To assess reproducibility, the experiment was performed in triplicate. Since phenol and SiNPs could be chemically altered at pH higher than 10, pH values 3-10 were only considered. Thus, study in this section aimed to find the optimal pH that gives the highest possible adsorption efficiency of modified SiNPs for removing phenol from aqueous medium. We found that the adsorption efficiency of phenol by SiNPs is significantly dependent on the solution pH such that decrease in the adsorption efficiency is observed above pH 7, while the increase in the adsorption efficiency is observed at pH 3-7. This indicates that an optimum pH value lies within pH 6-7, which can be explained concerning the effect of pH on the surface chemistry of modified SiNPs in aqueous solution.

The surface amino groups on the SiNPs play an important role in the adsorption process. To explore the pH effect on the efficiency of adsorption process, zeta potential was measured at different pH intervals. The surface modification of the nanomaterial using APTS was found adequate to yield a net positive surface charge at approximately +49 mV at pH 7. Further, in acidic medium, at pH 3, build-up of positive charge on the surface of the modified particles led to an increase in zeta potential to +56 mV. The high positive value of the zeta potential can be related to the accumulation of protons in the solution causing protonation of amino groups, thereby facilitating introduction of more positive ions onto the SiNPs surface. This, in turn, induces the electrostatic interactions with the negatively charged surface of phenolate ions accelerating adsorption of phenol. Note that the phenol molecules dissociate in basic aqueous solution at pKa=9.95 to yield phenoxide ions which are stabilized to some extent, resulting in deactivating the adsorption process due to probably repulsive forces between the negative charged in the surface of SiNPs and phenoxide ions; while in acidic conditions the presence of net positive charge on the surface of the modified SiNPs leads to electrostatic interaction with the phenolate ions and enhances the adsorption process. This is largely in good agreement with previous studies [6,55,56]. In basic media at pH 10, nanomaterials retain zeta potentials of −40 mV, where all the amino groups are converted into the deprotonated form, thereby affecting the removal efficiency of the adsorbate. Thus, decrease in the removal efficiency is observed due increase of the repulsion forces between the negative SiNPs surfaces and the phenol molecules, which leads to a low degree of adsorption. The phenol removal efficiency by AMS-10 is higher than that of AMS-20, AMS-30 and AMS-40 for the same pH values. This can be attributed to the smaller particle size of the AMS-10 sample bearing a higher surface area and subsequently providing more adsorption sites for the phenol ions.

3-3. Investigating the Effect of Initial Concentration

The influence of the initial phenol ion concentration on the effi-

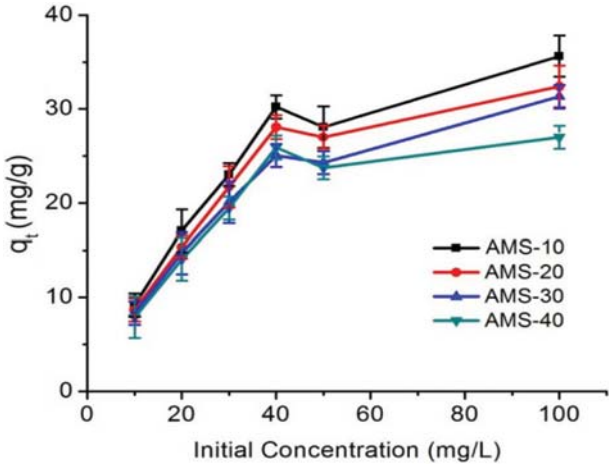

Fig. 5. Initial concentration influence on adsorption of phenol using SiNPs (Contact time=18 h, adsorbent dosage=1 mg/1 mL and pH: 7).

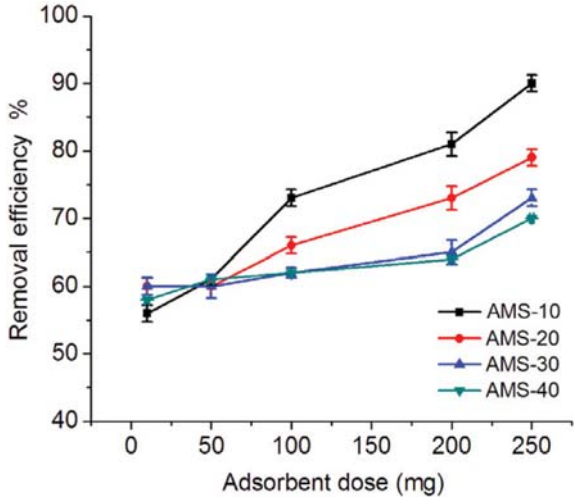

Fig. 6. Influence of adsorbent dosage on the phenol removal by SiNPs. Experimental conditions: Co.=10 mg/L; pH: 7 and contact time 18 h.

ciency of adsorption process was investigated as a function of the initial concentration to determine the relationship between the amount of phenol ions adsorbed on the adsorbent surface and the concentration of the remaining phenol ions in the aqueous phase. Fig. 5 shows the adsorption percentage of phenol ions with the initial phenol ions concentration (10-100 mg/L), while all the other factors were maintained constant. The adsorption efficiency of adsorbent decreases with the initial concentration of phenol. This could be explained by the limited active adsorption sites on the SiNPs surfaces with the high initial concentration of phenol in aqueous media, and thus a reduced removal efficiency because of the expected longer time required achieving the adsorption equilibrium at a higher phenol concentration [55,57,58]. Furthermore, the AMS-10 sample still showed a higher adsorption efficiency compared to other adsorbents at the same initial phenol concentration. The maximum removal efficiency of phenol was 85% at the initial concentration of 10 mg/L by AMS 10. This can be justified according to the smaller average particle size of the AMS-10 sample with the higher possible availability of active adsorption sites as well as a higher surface area of adsorbent.

3-4. Adsorbent Dose Effect

The adsorbent dose influence on the phenol ions removal efficiency on SiNPs was studied. The doses of the SiNPs were varied from 10 to 250 mg/25 mL, while the other factors, including pH, contact time, and initial concentration of phenol, were kept constant at 10 mg/L, 18 h and 7, respectively. As shown in Fig. 6(a), the increment of the absorbent dosage from 10 to 250 mg/25 mL led to a gradual enhancement in the adsorption percentage of phenol. This enhancement in the SiNPs dosage possibly led to an increase in the available active adsorption sites on the adsorbent surface; hence, an improved phenol removal was achieved.

3-5. Adsorption Capacity

The equilibrium adsorption capacity is a critical factor that affects the adsorption process; it detects the pollutant limit that can be extracted from an aqueous solution per adsorbent unit mass. The AMS-10 sample has the best adsorption capacity as a result of their improved physico-chemical characteristics, such as the specific surface area and the total volume of porosity. This facilitates ion migration into the interior of the composites, thereby enhancing the adsorption capacity of the pollutant [58,59]. Langmuir and Freundlich isotherm models are usually used to illustrate the distribution coefficient of adsorbates between the liquid and solid phases in the adsorption process. The obtained results of adsorption equilibrium, studied by the ratio of adsorbate mass that adsorbed to definite weight of the adsorbent and the adsorbate concentration at liquid phase equilibrium, are expressed utilizing adsorption isotherms, which well interprets the adsorption systems [56].

The obtained results of the adsorption equilibrium were studied by the ratio of adsorbate mass (phenol) that adsorbed to the adsorbent weight (SiNPs) and the adsorbate concentration at equilibrium in a liquid phase. Which is expressed utilizing adsorption isotherms and well interpreted the adsorption systems. The resulting data obtained on the adsorption process of phenol molecules on the surface of modified SiNPs were studied using the Langmuir and Freundlich isotherm models. From Fig. 7(a), the isotherm data have been linearized using Langmuir and Freundlich equations. Values of K_L and Q_{max} for the adsorption of phenol on SiNPs as calculated from Langmuir isotherm model are provided (see Table 3). The adsorption capacity (Q_{max}) and K_L values were calculated to be 35.2 mg/g and 0.192 mg/L, respectively, for AMS-10, which is higher than the adsorption capacity of non-amino modified SiNPs (16.4 mg/g) and other absorbents (see Table 4).

The Q_{max} and K_L values are clearly in good agreement with those observed experimentally. The enhanced adsorption capacity of AMS-10 can be attributed to the higher surface area, thereby higher total pore size to volume ratio of the particles, which increases the availability of active adsorption sites per volume ratio. This leads to a greater availability of active adsorption sites such that phenol ions can penetrate deeper into the surface pores of the silica layer. In addition to improving the surface characteristics as a result of amino modification of the SiNPs surface probably played an important role in the phenol adsorption due to the net of positive charge

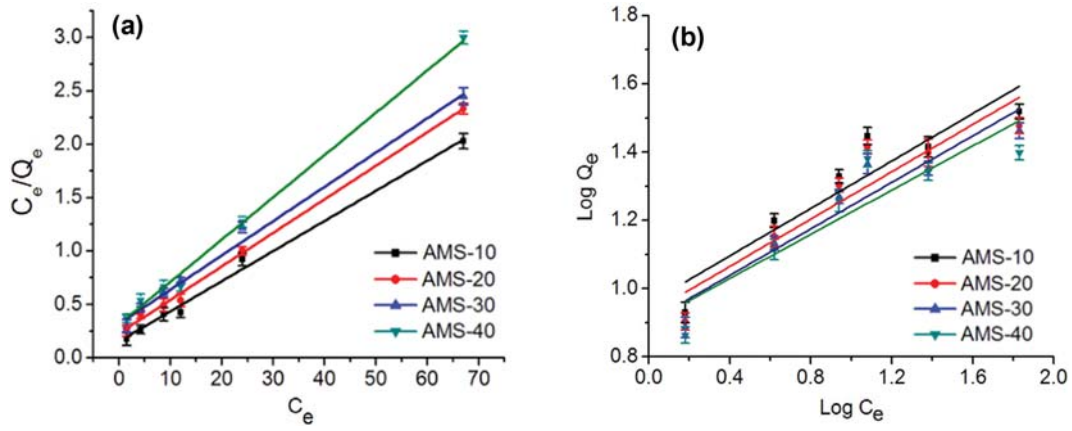

Fig. 7. (a) Langmuir and (b) Freundlich adsorption isotherm models.

Table 3. Parameters of Langmuir and Freundlich adsorption isotherm models

Adsorbent	Langmuir			Freundlich		
	Q_{max} (mg/g)	K_L (L/mg)	R^2	n	K_F	R^2
AMS-10	35.199	0.190	0.993	2.875	9.050	0.837
AMS-20	31.696	0.144	0.997	2.884	8.439	0.836
AMS-30	31.075	0.097	0.991	2.934	7.988	0.872
AMS-40	24.919	0.134	0.995	3.088	7.945	0.777

Table 4. Comparison of adsorption capacities of phenol using different adsorbents

Adsorbent	Q_{max} (mg/g)	Ref.
Amino modified SiNPs	35.20	Present study
Non-amino modified SiNPs	16.4	Present study
Fly ash	6.66	[60]
Surfactant-modified natural zeolite	0.76-1.30	[61]
Activated coal	1.48	[62]
Bamboo cellulose nanofibers-graft-poly (acrylic acid)	0.91	[63]
Bamboo cellulose nanofibers graft-poly (acrylic acid)/Sodium humate	1.02	[64]
Bamboo cellulose nanofibers	0.39	[64]
Activated carbon-commercial grade (ACC)	30.22	[64]
Activated carbon-laboratory grade (ACL)	24.65	[65]
Rattan sawdust based activated carbon	149.25	[65]
Functionalized silica based post synthesis grafting	30.8±2.2	[32]

on the SiNPs surface as a result of the accumulation of protons in the solution causing protonation of amino groups, thereby enhancing adsorption capacity of phenol. R^2 values of Langmuir model were 0.993, 0.997, 0.991 and 0.995 for AMS-10, AMS-20, AMS-30 and AMS-40, respectively. The values of R^2 are all larger than 0.99, indicating that the adsorption of phenol on SiNPs correlates well with the Langmuir model.

Adsorption isotherms of phenol removal efficiency by silica nanoparticles were also investigated and linearized using the Freundlich model (Fig. 7(b)). The Freundlich constants, K_F and n for the experimental data are shown in Table 3. The value of the correlation coefficient (R^2) was found to be 0.83, 0.83, 0.85 and 0.77 for AMS-10, AMS-20, AMS-30 and AMS-40, respectively. It is observed that the adsorption isotherms successfully fit the Langmuir isotherm model, and the adsorption behavior of phenol removal on silica nanoparticles is better depicted by the Langmuir adsorption model than the Freundlich model.

3-6. Kinetics of the Adsorption of Phenol onto SiNPs

The influence of contact time on the adsorption process of phenol molecules on the surface of the modified SiNPs (adsorbent) was investigated using the collected data in Fig. 3. It is observed that the absorption of phenol molecules on nanoparticles' surface was gradually increased and then it attains equilibrium at approximately 1,080 min. The kinetic analyses of the experimental data were studied by two common adsorption kinetic models (pseudo-first order and pseudo-second order). These kinetic models are

Table 5. Pseudo-first and pseudo-second-order models of the adsorption of phenol using SiNPs

SiNPs	Experimental value q_e (mg g^{-1})	First-order			Second-order		
		K_1	q_e	R^2	K_2	q_e	R^2
AMS-10	8.85	0.0014	7.19	0.662	0.0007	9.517	0.960
AMS-20	7.25	0.0012	3.61	0.865	0.0017	7.573	0.991
AMS-30	6.65	0.0011	2.92	0.969	0.002	6.943	0.994
AMS-40	6.3	0.0012	2.05	0.961	0.0033	6.533	0.998

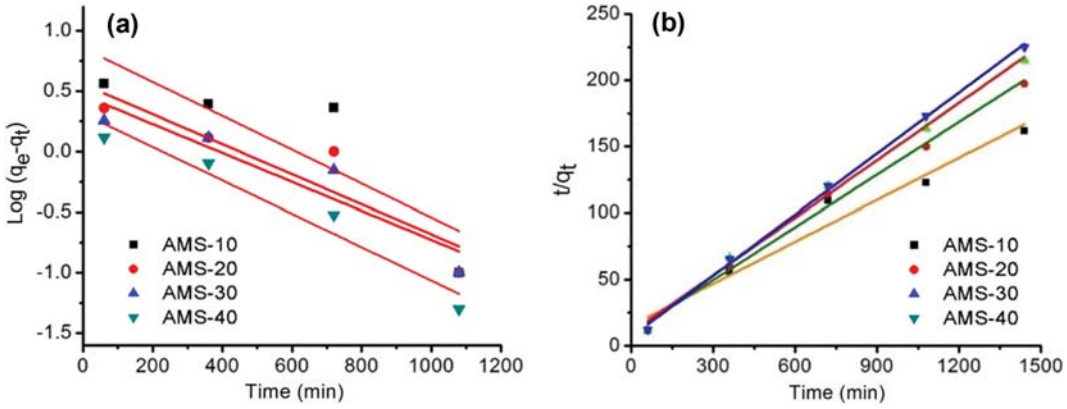

Fig. 8. (a) Pseudo-first and (b) pseudo-second-order kinetic models for the adsorption of Phenol onto SiNPs.

used to estimate the rate and the possible adsorption mechanism of phenol molecules on the modified surface of SiNPs (Table 5).

The pseudo-first-order [66] is described according to the following equation:

$$\text{Log}(q_e - q_t) = \log q_e - k_1 t$$

where q_e (mg/g) and q_t (mg/g) represent the adsorbed amounts of Phenolat equilibrium and time t (min), respectively. k_1 (min^{-1}) is the pseudo-first order rate constant. Fig. 8 shows the linear plots of log ($q_e - q_t$) versus (t) time consumed in the adsorption process of phenol onto SiNPs adsorbent.

The rate constants (K_1) and the theoretical adsorption capacities (q_e) were calculated from the slopes and intercepts, respectively, and their values are listed in Table 5.

Additionally, the linear formula of pseudo-second order model [67] is described as follows:

$$t/q_t = 1/k_2 q_e^2 + t/q_e$$

where k_2 (g mg^{-1} min^{-1}) is the rate constant of pseudo-second order. As shown in Fig. 3 the plots of t/q_t against t produce straight lines with slopes and intercepts corresponding to the pseudo-second-order rate constants (k_2) and the theoretical adsorption capacities $(q_e)_{theo}$, respectively. By comparing the values of correlation coefficients (R^2) and the theoretical adsorption capacities $(q_e)_{theo}$ of the pseudo-first and pseudo-second-order models (Table 5), it is noticed that R^2 values of pseudo-second order are higher than that of pseudo-first order and also, the values of $(q_e)_{theo}$ are in agreement with the experimental values. Thus, the obtained results of adsorption kinetics were found to follow the pseudo-second-order kinetic model. The results found that Langmuir model was established to be more proper to designate the adsorption of phenolate ions onto surface of amino modified silica nanoparticles. AMS-10 has the highest adsorption capacity, which can be attributed to higher specific surface area and the presence of maximum amino groups. Recently, there has been much effort to investigate the relation between the Lagergren (first-order rate equation), second-order rate equation and Langmuir adsorption isotherm for the batch method experiment. These efforts end with a significant procedure which allows the transformation of adsorption rate equation for batch adsorption, conforming the Langmuir kinetics to a linear combination of a first-order and a second-order equation is defined [68]. Moreover, the rate of the reaction not only depends on the amount of amino modified silica nanoparticles but also on the amount of adsorbed phenol molecules on the surface of the nanoparticles at equilibrium.

CONCLUSION

The work shows that the amino-modified SiNPs are effective adsorbents for phenol ion removal from aqueous media. Modification of the SiNPs results in positively charged surface particles that can be easily adsorbed to negatively charged contaminants. This constitutes a straightforward and novel utility to remove one of the most dangerous water contaminants that can be used for a wide range of pollutants. The SiNPs were synthesized in the range of 10 to 40 nm average diameter and labeled as (AMS-10 to 40); the surface was modified using APTS with the one-pot Stöber method. The synthesized nanoparticles were characterized based on their size and surface chemistry using TEM, DLS, zeta potential, elemental analyses, TGA and FTIR. The removal efficiency of the synthe-

sized nanomaterial was found to be size dependent, where smaller particle size has a larger surface area to volume ratio. The adsorption capacity of AMS-10 was higher than other adsorbents under the same conditions, where the Q_{max} and K_L values were calculated to be 35.2 mg/g and 0.192 mg/L, respectively. For the phenol adsorption efficiency, the phenol adsorption capacity was in the following order: AMS-10>AMS-20>AMS-30>AMS-40. Interestingly, the adsorption efficiency of phenol by SiNPs was found to be considerably pH-dependent. Langmuir and Freundlich isotherm models were utilized to illustrate the adsorption equilibrium of phenol onto the modified SiNPs. The linear regression of the experimental data showed that the Langmuir adsorption model better explains the adsorption behavior of phenol removal on silica nanoparticles than the Freundlich model. The kinetic analyses of the adsorption processes were studied, and the data show that the reaction rate is a pseudo-second-order reaction. The study, therefore, frames out a simple set-up and a versatile strategy that can provide a highly compatible method for removing phenol from contaminated water.

REFERENCES

1. L. Zhang, J. Liu, C. Tang, J. Lv, H. Zhong, Y. J. Zhao and X. Wang, *Appl. Clay Sci.*, **51**, 68 (2011).
2. T. O. Said, R. S. Farag, A. M. Younis and M. A. Shreadah, *Bullet. Environ. Contam. Toxic.*, **77**, 451 (2006).
3. (a) A. M. Younis and S. M. Nafea, *World Appl. Sci. J.*, **19**, 1423 (2012); (b) B. Gulay, A. Aydin and A. M. Yakup, *J. Hazard. Mater.*, **244**, 528 (2013).
4. G. Busca, S. Berardinelli, C. Resini and L. Arrighi, *J. Hazard. Mater.*, **160**, 265 (2008).
5. Federal Register, Environmental Protection Agency, Part VIII, 40 CFR Part **136**, 58 (1984).
6. Z.-A. Mirian and A. Nezamzadeh-Ejhieh, Desalination and Water Treatment, 1 (2015).
7. M. A. Shannon, P. W. Bohn, M. Elimelech, J. G. Georgiadis, B. J. Mariñas and A. M. Mayes, *Nature*, **452**, 301 (2008).
8. A. B. Dichiara, S. J. Weinstein and R. E. Rogers, *Ind. Eng. Chem. Res.*, **54**(34), 8579 (2015).
9. P. Canizares, M. Carmona, O. Baraga and M. A. Rodrigo, *J. Hazard. Mater.*, **131**, 243 (2006).
10. A. Dabrowski, P. Podkoscielny, Z. Hubicik and M. Barczak, *Chemosphere*, **58**, 1049 (2005).
11. Z. Lazarova and S. Boyadzhieva, *Chem. Eng. J.*, **100**, 129 (2004).
12. Y. A. Alhamed, *Bulg. Chem. Comm.*, **40**, 26 (2008).
13. F. A. Banat, B. Al-Bashir, S. Al-Asheh and O. Hayajneh, *Environ. Pollut.*, **107**, 391 (2002).
14. S. Nomanbahay and K. Palanisamy, *Electron. J. Biotechnol.*, **8**, 43 (2005).
15. N. S. Alderman, A. L. N'Guessan and M. C. Nyman, *J. Hazard. Mater.*, **146**, 652 (2007).
16. N. Sona, T. Yamamoto, D. Yamamoto and M. Nakaiwa, *Chem. Eng. Process.*, **46**, 513 (2007).
17. S. Hydari, H. Sharififard, M. Nabavinia and M. Reza, *Chem. Eng. J.*, **193**, 276 (2012).
18. K. Bhattacharyya and S. Gupta, *Colloids Surf., A*, **277**, 191 (2007).
19. K. A. Halouli and N. M. Drawish, *Sep. Sci. Technol.*, **30**, 3313 (1995).
20. S. Mitra, Sample Preparation Techniques in Analytical Chemistry, Wiley, Hoboken, New Jersey (2003).
21. D. K. Singh and B. Srivastava, *J. Sci. Ind. Res.*, **61**, 208 (2002).
22. S. Kulkarni and J. Kaware, *Int. J. Sci. Eng. Res.*, **1**, 88 (2013).
23. A. M. Younis, E. M. A. Nafea, Y. Y. I. Mosleh and M. S. Hefnawy, *J. Medit. Ecol.*, **14**, 55 (2016).
24. F. Ektefa , S. Javadian and M. Rahmati, *J. Taiwan Inst. Chem. Engineers*, **88**, 104 (2018).
25. N. Tancredi, N. Medero, F. Moller, J. Piriz, C. Plada and T. Cordero, *J. Colloid Interface Sci.*, **279**, 357 (2004).
26. K. Yang, W. Wu, Q. Jing and L. Zhu, *Environ. Sci. Technol.*, **42**, 7931 (2008).
27. B. Pan, W. Zhang, Q. Zhang and S. Zheng, *J. Hazard. Mater.*, **157**, 293 (2008).
28. I. Vázquez, J. Rodriguez-Iglesias, E. Maranon, L. Castrillon and M. Alvarez, *J. Hazard. Mater.*, **147**, 395 (2005).
29. Z. U. Ahmad, Q. Lian, M. E. Zappi, P. R. Buchireddy and D. D. Gang, *J. Environ. Sci.*, **75**, 307 (2019).
30. Y. Ku and K. C. Lee, *J. Hazard. Mater. B.*, **80**, 59 (2000).
31. A. Chen, Y. Li, Y. Yu, Y. Li, K. Xia, Y. Wang, S. Li and L. Zhang, *Carbon*, **103**, 157 (2016).
32. M. Ebrahimi-Gatkash, H. Younesi, A. Shahbazi and A. Heidari, *Appl. Water Sci.*, **7**(4), 1887 (2017).
33. K. H. Radeke, D. Loseh, K. Struve and E. Weiss, *Zeolites*, **13**, 69 (1993).
34. S. Kim and E. Marand, *Micropor. Mesopor. Mater.*, **114**, 129 (2008).
35. V. M. Martínez, V. P. Sánchez and J. M. M. Martínez, *Eur. Polym. J.*, **44**, 3146 (2008).
36. S. Shiomi, M. Kawamori, S. Yagi and E. Matsubara, *J. Colloid Interface Sci.*, **460**, 47 (2015).
37. C. Chen, R. S. Justice, D. W. Schaefer and J. W. Baur, *Polymer*, **49**, 3805 (2008).
38. S. M. C. Ritchie, L. G. Bachas, T. Olin, S. K. Sikdar and D. Bhattacharyya, *Langmuir*, **15**, 6346 (1999).
39. S. V. Mattigod, X. Feng, G. E. Fryxell, J. Liu and M. Gong, *Sep. Sci. Technol.*, **34**, 2329 (1999).
40. W. Yantasee, Y. Lin, G. E. Fryxell, B. J. Busche and J. C. Birnbaum, *Sep. Sci. Technol.*, **38**, 3809 (2003).
41. S. Iwamoto, W. Tanakulrungsank, M. Inoue, K. Kagawa and P. Praserthdam, *J. Mat. Sci. Lett.*, **19**, 1439 (2000).
42. S. M. Saleh, R. Müller, H. S. Mader, A. Duerkop and O. S. Wolfbeis, *Anal. Bioanal. Chem.*, **398**, 1615 (2010).
43. H. S. Mader, X. Li, S. M. Saleh, M. Link, P. Kele and O. S. Wolfbeis, *Ann. N. Y. Acad. Sci.*, **1130**, 213 (2008).
44. W. Stöber and A. Fink, *J. Colloid Interface Sci.*, **26**, 62 (1968).
45. (a) D. E. Achatz, F. J Heiligtag, X. Li, M. Link and O. S. Wolfbeis, *Sens. Act. B: Chem.*, **150**, 211 (2010); (b) R. Ali, S. M. Saleh and R. F. M. Elshaarawy, *RSC Adv.*, **6**(90), 86965 (2010).
46. Malvern Instruments Ltd., https://www.malvernpanalytical.com/en. Accessed February 2019.
47. Jasco Inc. http://www.jascoinc.com/spectroscopy/ft-ir-4000-series. Accessed February 2019.
48. R. W. Martin, *Analyt. Chem.*, **21**, 1419 (1949).
49. M. Qhobosheane, S. Santra, P. Zhang and W. Tan, *Analyst*, **126**, 1274 (2001).
50. S. Bhakta, C. K. Dixit, I. Bist, K. A. Jalil, S. L. Suib and J. F. Rusling,

Mater. Res. Express, **3**(7), 075025 (2016).
51. U. Thawornchaisit and K. Pakulanon, *Bioresour. Technol.*, **98**, 140 (2007).
52. A. Bhatnagar, *J. Hazard. Mater.*, **139**, 93 (2007).
53. N. F. Zainudin, A. Z. Abdullah and A. R. Mohamed, *J. Hazard. Mater.*, **174**, 299 (2010).
54. S. J. Allen, Q. Gan, R. Matthews and P. A. Johnson, *J. Colloid Interface Sci.*, **286**, 101 (2005).
55. H. A. Asmaly, B. Abussaud, T. A. Saleh, V. K. Gupta and M. A. Atieh, *J. Saudi Chem. Soc.*, **19**, 511 (2015).
56. G. Yang, L. Tang, G. Zeng, Y. Cai, J. Tang, Y. Pang, Y. Zhou, Y. Liu, J. Wang, S. Zhang and W. Xiong, *Chem. Eng. J.*, **259**, 854 (2015).
57. A. M. Younis, A. V. Kolesnikov and A. V. Desyatov, *Am. J. Anal. Chem.*, **5**(17), 1273 (2014).
58. M. Anbia and S. Khoshbooei, *J. Nanostruct. Chem.*, **5**, 139 (2005).
59. Y. F. Lin and J. L. Chen, *J. Colloid Interface Sci.*, **420**, 74 (2014).
60. S. Kumar, S. N. Upadhyay and Y. D. Upadhya, *Chem. Tech. Biotechnol.*, **37**, 281 (1987).
61. A. Kuleyin, *J. Hazard. Mater.*, **144**, 307 (2007).
62. P. Pal and R. Kumar, *Sep. Purif. Rev.*, **43**(2), 89 (2014).
63. X. Zhang, J. Zhao, L. Cheng, C. Lu, Y. Wang, X. He and W. Zhang, *RSC Adv.*, **4**, 55195 (2015).
64. V. C. Srivastava, M. M. Swamy, I. D. Mall, B. Prasad and I. M. Mishra, *Colloids Surf., A: Physicochem. Eng. Aspects*, **272**, 89 (2006).
65. B. H. Hameed and A. A. Rahman, *J. Hazard. Mater.*, **60**, 576 (2008).
66. H. Yuh-Shan, *Scientometrics*, **59**(1), 171 (2004).
67. Y. S. Ho, *Water Res.*, **40**(1), 119 (2006).
68. C. Tien and B. V. Ramarao. *Sep. Purif. Technol.*, **136**, 303 (2014).